

Virtual synchronous machine control of grid connected power electronic converters for power system applications

Kumaravel S.*, Vinu Thomas*, Terence O'Donnell** and Ashok S.*

*National Institute of Technology Calicut, Kerala, India

**University College Dublin, Belfield, Dublin, Ireland

*Corresponding Author: kumaravel_s@nitc.ac.in

ABSTRACT

Renewable energy based distributed power generators are becoming an integral part of future power systems. Power electronic converters have a major role as the interface device between the renewable energy sources and the utility grid. Since the power electronic converters do not possess any rotating inertia like a synchronous generator, rapid fluctuations in power supply and demand cause sudden deviations in the frequency of power electronic converter dominated weak grids. A virtual synchronous machine (VSM) approach for controlling the inverters connected to the grid attempts to imitate the behaviour of a synchronous machine and provides virtual inertia to the grid by virtue of the electric storage. In this paper a modified VSM control strategy based on swing equation is proposed for three-phase grid connected inverters. The proposed control strategy is implemented in stationary reference frame and does not need a phase locked loop for grid synchronization unlike many of the existing methods reported in the literature. The VSM unit consists of a DC storage unit connected through a three-phase voltage source converter with an *LCL*-filter into the grid and the corresponding local control system. A test setup of the VSM unit with the specification of 200 V, 50 Hz, 1 kVA is developed in laboratory environment to validate the control scheme. Different performance studies such as real and reactive power control of VSM, effect of variation in the value of inertia of VSM on the power response, and response of VSM for the grid frequency variation have been carried out. The performance of VSM control is compared with the conventional droop control method for the grid connected converters. The results prove that the modified VSM control scheme gives better performance than the conventional droop control.

Keywords: Virtual synchronous machine; virtual inertia; real time simulator.

INTRODUCTION

Pollution caused due to the combustion of fossil fuels in conventional power generating stations and the diminishing gap between the supply and demand of fossil fuels are two major factors that have given a major impetus towards the utilization of renewable energy in the last few decades. Due to the intermittency of the renewable sources like solar and wind energy, power electronic converters like inverters form a crucial interface between the renewable sources and the utility grid. The percentage share of converter based renewable energy generation in the power system network increases at an exponential rate in most countries due to the government policies for promoting renewable energy utilization. Microgrid concept for power generation and distribution is popular in the last two decades as a promising model for future power systems.

A microgrid is capable of operating in islanded mode in addition to the grid connected mode of operation. In islanded mode of operation, the inverter based distributed generators have the additional role of maintaining the stability of the microgrid. The stability analysis of inverter based microgrids requires the development of the small signal state space model of the microgrid to properly design the controller parameters (Pogaku et al., 2007). Adaptive controllers along with efficient communication networks can help the inverters in the microgrid to return to normal

operating conditions after transients (Bidram et al., 2014). But, still the lack of inertia in inverter based microgrids causes serious transient stability issues (Tielens et al., 2016). Provision of imparting virtual inertia to inverters by using electrical energy storage available at the DC link is considered as a promising solution for the frequency stability issues in microgrids (Pertl et al., 2017).

A control strategy based on the emulation of a synchronous generator was proposed by Beck and Hesse (2007) for inverters operating in weak grids, which is named Virtual Synchronous Machine (VISMA) concept by the authors. The unique feature of this control strategy is that it combines the merits of an inverter with the static and dynamic properties of a synchronous generator. But since a full order model of a synchronous generator is required for the controller, it makes the overall control scheme complex. The Virtual Synchronous Generator (VSG) concept was proposed by Driesen and Visscher (2008), which imparts virtual inertia to an inverter with the help of short term energy storage. This idea increases the grid stability for the power electronic converter based microgrids. The limitations on the penetration level of power electronic interfaced generators in the utility grid can be removed using this type of control.

The Synchronverter concept, which mimics the behaviour of synchronous generators in an inverter, was proposed by Zhong and Weiss (2011). When compared to the VISMA concept, the performance of a synchronverter is not affected by the tracking error of the currents and voltages. But the synchronverter control scheme needed a Phase Locked Loop (PLL) to synchronize the inverter with the grid whenever it moves from islanded mode to grid connected mode. Self synchronized synchronverter was proposed by Zhong et al. (2014), which does not need a PLL for its synchronization with the grid.

State space model of a virtual synchronous machine (VSM) implementation with cascaded voltage-current control loop is developed by D'Arco et al. (2015). The stability assessment is conducted using the eigenvalues of the small signal model and their parametric sensitivities. The linearized small signal model of the VSM operating in islanded mode and the design of VSM parameters based on small signal models are presented by Wu et al. (2016). An enhanced VSM strategy is proposed to solve the issues of active power oscillation and improper transient active power sharing in parallel VSM controlled inverters by adapting the virtual stator reactance based on state space analysis (Liu et al., 2017). An algebraic VSM proposed by Hirase et al. (2018) with a minimum number of parameters was used to suppress the frequency and voltage deviations in microgrids.

A self tuning algorithm for finding the optimum parameters of the VSM for minimizing the amplitude, the rate of change of frequency values, and power transfer from energy storage is proposed in Torres et al. (2014). The self tuning VSM was found to give similar performance as that of constant parameters VSM with lesser power consumption from energy storage. Instead of using a constant value of the moment of inertia in a VSM, its value is switched between a small value and a large value based on the feedback signals (Alipoor et al., 2015). By alternating the moment of inertia between the small and large values, the frequency and power oscillations were found to be damped. Guan et al. (2015) proposes a synchronous generator emulation control scheme for Voltage Source Converter (VSC) - HVDC station. The VSM control has been implemented in a single phase grid connected solar-PV inverter with battery storage in Mishra et al. (2016). Since DC microgrids are gaining popularity these days, the possibility of the DC microgrid integration as VSM into the utility grid has also been explored (Chen et al., 2017).

This paper focuses mainly on developing a VSM control for power electronic converters, which are used in power system applications. The basic swing equation of a synchronous machine is used to impart virtual inertia properties to the converter without the need for a PLL. The objectives of this work are as follows: a) Modelling, simulation, and performance evaluation of VSM control; b) Implementation of VSM control on a real time simulator; c) Performance evaluation and comparison with existing droop control method.

VIRTUAL SYNCHRONOUS MACHINE CONTROL

A three-phase inverter along with an *LCL* filter, DC source, or energy storage and the associated VSM based controller, which controls the gate pulses of the inverter, can be considered as a VSM as shown in Figure 1. The VSM is connected to the grid using a static switch, *S*. The *LCL* filter is used to filter out the harmonic contents present in the output of the inverter to give a sinusoidal current at the Point of Common Coupling (PCC). The voltage and current signals from the PCC are measured and these signals are used by VSM controller to generate the gate pulses to operate

the inverter. The inverter is capable of operating with bidirectional power flow; i.e., it can inject power into the grid or absorb power from the grid depending on the operating conditions.

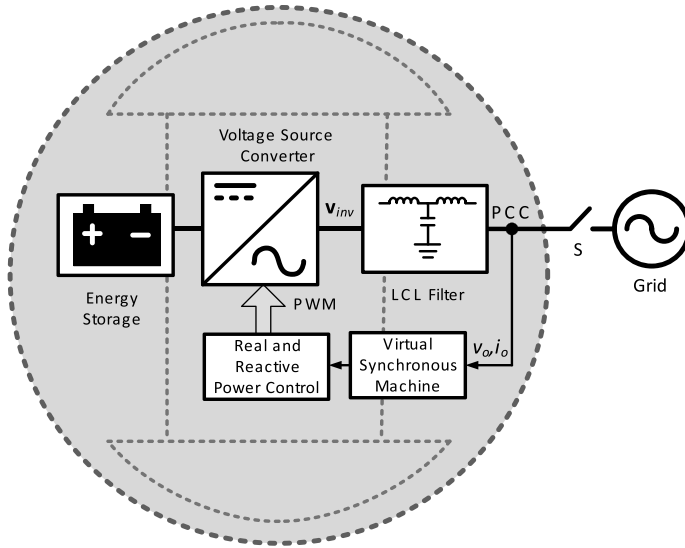


Fig. 1. Block diagram of VSM connected to grid.

The VSM control operates based on the synchronous machine’s swing equation to emulate its virtual inertia property. According to the rotor motion equation of the synchronous machine, the acceleration of the virtual machine speed is determined by the power balance equation as follows:

$$T_a \frac{d\omega_{VSM}}{dt} = P_m - P_e + k_w(\omega_{VSM}^* - \omega_{VSM}) - k_d(\omega_{VSM} - \omega_{grid}) = P_{VSM} \quad (1)$$

where T_a is the inertia constant, ω_{VSM} is the angular speed of the VSM, P_m is the virtual input mechanical power, P_e is the measured electrical power injected to the grid from VSM, ω_{VSM}^* is the reference angular speed of the VSM, ω_{grid} is the angular speed of the grid, k_d is the damping constant, k_w is the droop constant, and P_{VSM} is the output power reference of the VSM. Rearranging and integrating Equation (1), we get

$$\omega_{VSM} = \frac{1}{T_a} \int P_{VSM} dt \quad (2)$$

The VSM control strategy is basically developed from Equation (1) and Equation (2). The schematic diagram of VSM control is shown in Figure 2.

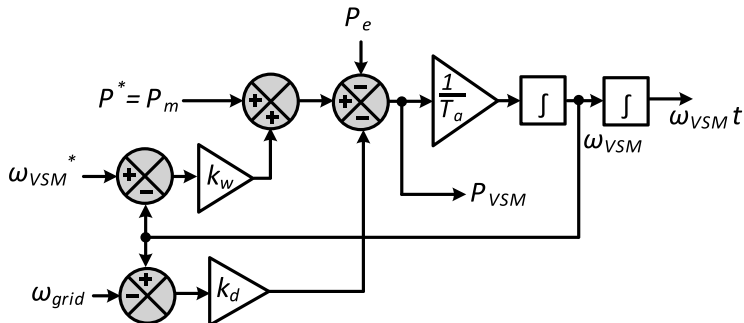


Fig. 2. Schematic diagram of VSM control.

Figure 3 shows the block diagram of the real and reactive power control of VSM. The power fed by the VSM is controlled by a PI controller, which keeps the actual power fed by VSM to the reference real power by adjusting the phase angle of the modulating sine wave as given in Equation (3). Similarly, the magnitude of modulation voltage is derived from reactive power as given in Equation (4).

$$\delta = \left(K_{p1} + \frac{K_{i1}}{s} \right) (P_{VSM} - P_e) \quad (3)$$

$$V_m = \left(K_{p2} + \frac{K_{i2}}{s} \right) (K_q(Q^* - Q_e) + V_{VSM}^*) \quad (4)$$

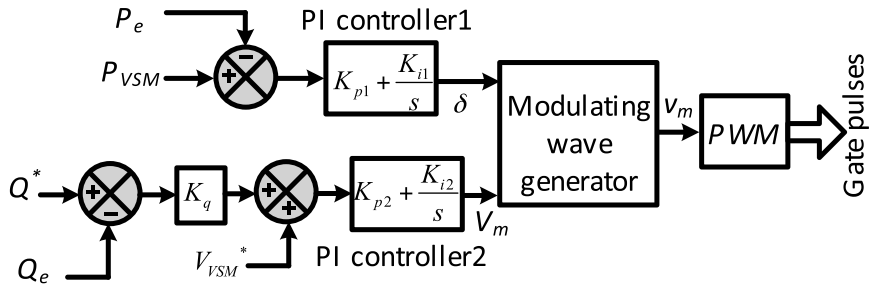


Fig. 3. Real and reactive power control of VSM.

P_{VSM} and Q^* are the reference real and reactive powers to the VSM. The reference reactive power is taken as zero in this work. When the reference real power is positive, VSM injects power into the grid and absorbs power from the grid when it is negative. By controlling the reference power, the amount of power from the DC side to the AC side of the inverter can be controlled using VSM. P_e and Q_e are the actual real and reactive power transferred between the VSM and the grid. The actual real and reactive powers are calculated from the measured three-phase voltages (v_o) and currents (i_o) at the PCC. Finally, the three-phase modulation voltages are calculated as given in Equations (5)-(7) and given to the PWM block for gate pulse generation to drive the IGBT switches in the inverter.

$$v_{ma} = V_m \sin(\omega_{VSM}t + \delta) \quad (5)$$

$$v_{mb} = V_m \sin(\omega_{VSM}t + \delta - 120^\circ) \quad (6)$$

$$v_{mc} = V_m \sin(\omega_{VSM}t + \delta - 240^\circ) \quad (7)$$

MATHEMATICAL MODEL AND STABILITY ANALYSIS

The mathematical modelling and stability analysis of the proposed control strategy are carried out using the small signal state space model of the VSM connected to the utility grid based on the methodology reported by D'Arco et al. (2015). The state space representation of the system consists of ten distinct state variables and four input signals. The state vector, \mathbf{x} , and input vector, \mathbf{u} , are defined by Equation (8) and Equation (9).

$$\mathbf{x} = [v_{od} \quad v_{oq} \quad i_{od} \quad i_{oq} \quad i_{invd} \quad i_{invq} \quad \xi \quad \gamma \quad \delta\omega_{VSM} \quad \delta\theta_{VSM}]^T \quad (8)$$

$$\mathbf{u} = [P^* \quad Q^* \quad \omega_{VSM}^* \quad V_{VSM}^*]^T \quad (9)$$

The non-linear state space model of the system is given by Equations (10)-(19) based on the overall system model as shown in Figures 1- 3.

$$\frac{dv_{od}}{dt} = \frac{1}{C_f} i_{invd} - \frac{1}{C_f} i_{od} + \omega_{VSM} v_{oq} \quad (10)$$

$$\frac{dv_{oq}}{dt} = \frac{1}{C_f} i_{invq} - \frac{1}{C_f} i_{oq} + \omega_{VSM} v_{od} \quad (11)$$

$$\frac{di_{od}}{dt} = \frac{1}{L_f} v_{od} + \frac{1}{L_f} V_{mo} \cos(\delta\theta_{VSM}) - \frac{R_f}{L_f} i_{od} - \omega_{VSM} i_{oq} \quad (12)$$

$$\frac{di_{oq}}{dt} = \frac{1}{L_f} v_{oq} + \frac{1}{L_f} V_{mo} \sin(\delta\theta_{VSM}) - \frac{R_f}{L_f} i_{oq} - \omega_{VSM} i_{od} \quad (13)$$

$$\frac{di_{invd}}{dt} = \frac{1}{L_f} v_{invd} - \frac{1}{L_f} v_{od} - \frac{R_f}{L_f} i_{invd} + \omega_{VSM} i_{invq} \quad (14)$$

$$\frac{di_{invq}}{dt} = \frac{1}{L_f} v_{invq} - \frac{1}{L_f} v_{oq} - \frac{R_f}{L_f} i_{invq} + \omega_{VSM} i_{invd} \quad (15)$$

$$\frac{d\xi}{dt} = P_{VSM} - v_{od} i_{od} - v_{oq} i_{oq} \quad (16)$$

$$\frac{d\gamma}{dt} = (Q^* + v_{od} i_{oq} - v_{oq} i_{od}) K_q + v_{vsm}^* \quad (17)$$

$$\frac{d\delta\omega_{VSM}}{dt} = \frac{P^*}{T_a} - \frac{(v_{od} i_{od} + v_{oq} i_{oq})}{T_a} + \frac{(k_\omega + k_d)}{T_a} (\omega_{VSM}^* - \omega_{VSM}) \quad (18)$$

$$\frac{d\delta\theta_{VSM}}{dt} = \delta\omega_{VSM} \quad (19)$$

Equation (18) is formulated from equation (1) with the assumption that the grid frequency, ω_{grid} , is approximately equal to ω_{VSM}^* during the steady state operation of the VSM control. In the state space model, v_o and i_o are the output voltage and current, respectively, at the PCC, i_{inv} is the output current of the inverter before the *LCL* filter, L_f and R_f are the values of the inductor used in the *LCL* filter, C_f is value of the filter capacitor, ξ represents the integrator output of the power controller, and γ represents the integrator output of the voltage controller. The real and reactive powers of the VSM are calculated using the voltage and current signals obtained in *d-q* from the *abc* frame. The inverter output voltage before the *LCL* filter is represented by \mathbf{v}_{inv} has the expression given in Equation (20).

$$\mathbf{v}_{inv} = v_{invd} + jv_{invq} = V_m \cos \phi + jV_m \sin \phi \quad (20)$$

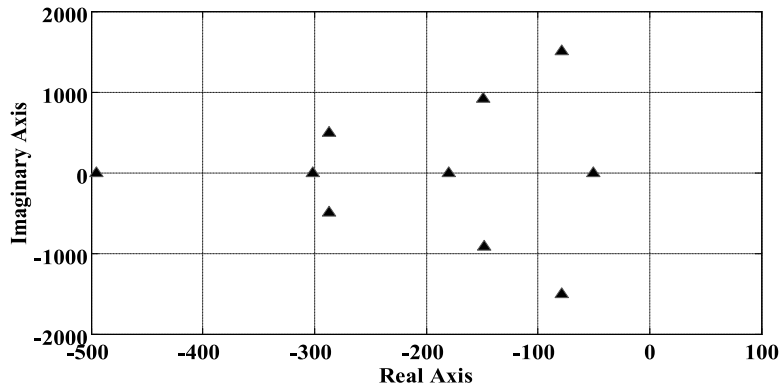
Since the Equations (10)-(20) are non-linear, the classical stability assessment methods cannot be directly applied. Therefore, a corresponding linearized small signal state space model is given by Equation (21).

$$\Delta \dot{\mathbf{x}} = \mathbf{A} \Delta \mathbf{x} + \mathbf{B} \Delta \mathbf{u} \quad (21)$$

The eigenvalues of the *A* matrix can be calculated to identify the oscillatory modes of the system. The resulting system eigenvalues are given in Table 1 and plotted as shown in Figure 4. Since the eigenvalues lie on the left side of the imaginary axis and far from the origin, the system can be considered as stable.

Table 1. System eigenvalues.

$\lambda_1 = -50.4$	$\lambda_6 = -148.8 - j 912.0$
$\lambda_2 = -301.2$	$\lambda_7 = -495.0$
$\lambda_3 = -78.7 + j 1510.0$	$\lambda_8 = -286.9 + j 498.0$
$\lambda_4 = -78.7 - j 1510.0$	$\lambda_9 = -286.9 + j 498.0$
$\lambda_5 = -148.8 + j 912.0$	$\lambda_{10} = -179.6$

**Fig. 4.** Eigenvalue plot.

SIMULATION OF VSM AND VALIDATION USING EXPERIMENTAL RESULTS

Based on the proposed mathematical model of the VSM, a simulation model is developed using MATLAB/Simulink to conduct various performance studies. Various parameters of the VSM used in the simulation are given in Table 2. For realising the feasible implementation of VSM based inverter control in the laboratory environment, the VSM is designed for a base power rating of 1 kVA. The line to line voltage of the AC side of the VSC converter is taken as 200 V RMS, 50 Hz. Frequency droop constant, k_w , and voltage droop constant, k_q , are given in per unit (p.u.) values.

Table 2. Specifications of VSM controlled grid connected inverter system.

Parameter	Value
Grid voltage (L-L)	200 V
Grid frequency	50 Hz
L_f & C_f	66 mH & 80 μ F
DC link voltage	360 V
Virtual inertia constant, T_a	2 s
Angular frequency of VSM, ω_{VSM}	314 rad/s
Frequency droop constant, k_w	20 p.u.
Voltage droop constant, k_q	0.2 p.u.
Switching frequency	1350 Hz

The VSM control algorithm is implemented in OPAL-RT[®] OP5700 real time simulator system to control a grid connected inverter set up in the laboratory. The DC source, the three-phase inverter, and the *LCL* filters are fabricated as per the specifications given in Table 2. The voltage and current signals from the VSM at the PCC are acquired and

fed to the real time simulator using OPAL-RT OP8660 data acquisition system. The data acquisition system senses currents and voltages at the PCC and converts them into analog signals with maximum amplitude of ± 10 V and fed to the real time simulator. The real time simulator runs the VSM control algorithm with the current and voltage signals at the PCC as feedback signals and generates six PWM gate pulses needed to drive the IGBT's in the VSM.

For validating the proposed control strategy for VSM simulation, hardware experimentations were conducted. The output current and voltage obtained during simulation and hardware experimentation are shown in Figure 5. The line current flowing through each phase at the PCC is shown in Figure 5 (a) and 5(b). The line to line voltage across all the phases at the PCC is shown in Figure 5 (c) and 5(d).

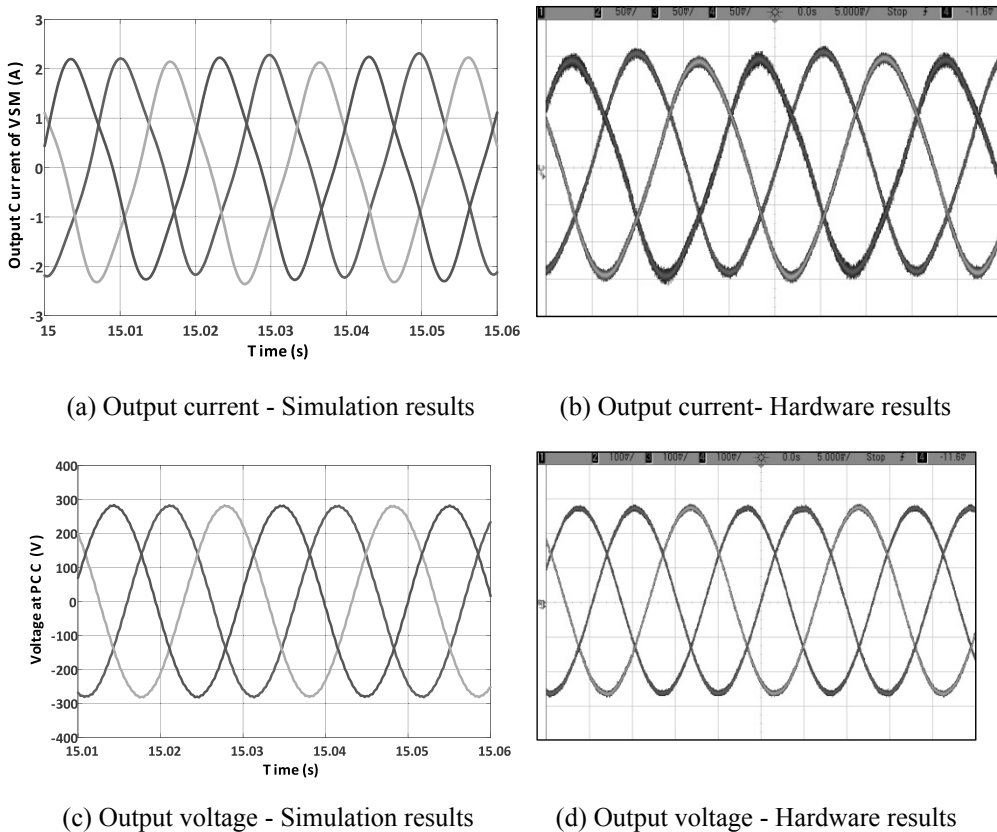


Fig. 5. Output current and voltage waveforms of VSM.

A. Response of VSM to the variation in grid frequency

At 2s, the grid frequency is reduced from 50 Hz to 49 Hz, and the corresponding variation in real power, reactive power, frequency of VSM, and grid frequency obtained in both simulation and experimentation are shown in Figure 6. From the figure, it is evident that when the grid frequency is reduced, there is no change in reactive power except a small deviation during the transient period. But the real power fed by the VSM to the grid increases, similar to the drooping characteristics of synchronous machine with governor mechanism. The grid frequency as measured by a PLL can be seen to be dropping from 50 Hz to 49 Hz and the VSM frequency is seen to follow the variation in grid frequency. The observed waveforms of both simulation and experimentation closely match with each other.

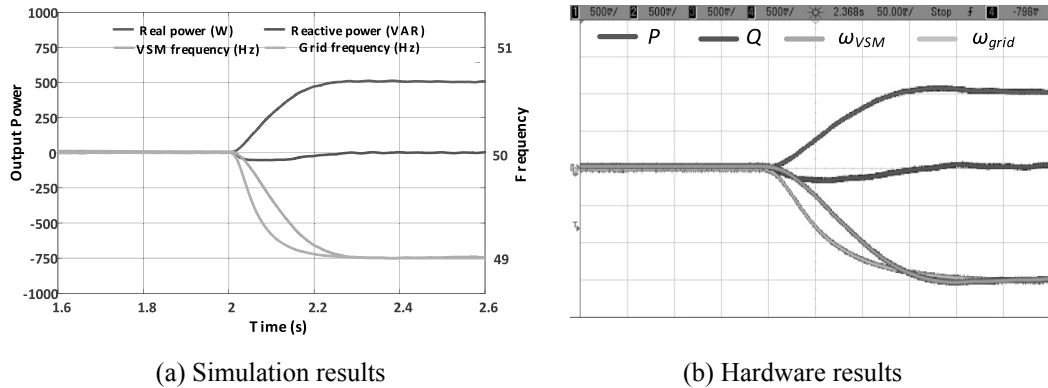


Fig. 6. Variation in real power, reactive power, grid frequency, and VSM frequency.

B. Response of VSM to the variation in real power reference

Performance of the VSM has been verified for transferring a real power of 500 W between the grid and VSM by giving the reference active power to the VSM. According to the reference real power, VSM injects or absorbs 500 W real power into or from the grid as shown in Figure 7(a). Initially transients can be observed in the real and reactive power during the synchronization process of VSM with grid, which is initiated at the instant t_1 . Whenever the reference active power changes, a small disturbance is observed in reactive power due to the coupling between active and reactive power. Figure 7(b) shows the real and reactive power control of VSM using reference values. In the first half of the waveform obtained from the DSO, a negative real power reference (-400 W) was given and then a positive real power reference (400 W) was given. Later on, a positive reactive power reference (400 VAR) was given and then a negative reactive power reference (-400 VAR) was given. Figure 7(b) proves the capacity of VSM to control the real and reactive power injection and absorption with the grid using external real and reactive power reference.

Figure 8(a) shows the voltage at PCC and the output current of phase ‘A’ during the power sharing of VSM with the grid. The output current of phase ‘A’ of VSM is in phase with the phase ‘A’ voltage at PCC when the power is injected from VSM. Similarly, it is 180° out of phase when the power is absorbed from the grid as shown in Figure 8(b).

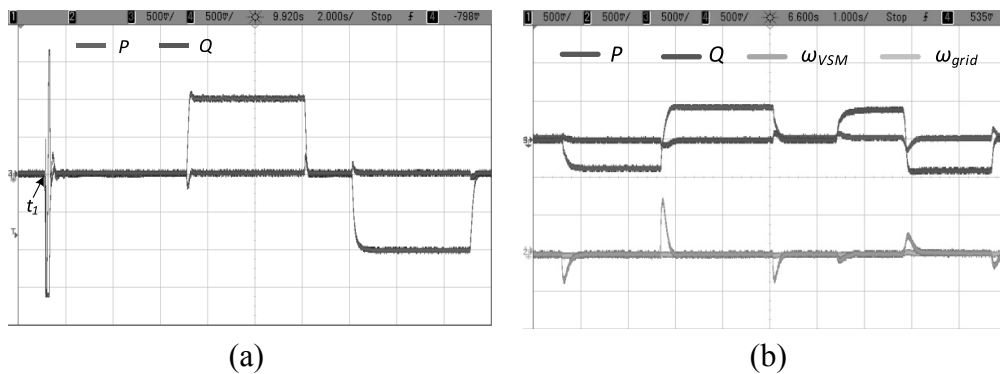


Fig. 7. (a) Active power control in VSM (b) ω_{VSM} and ω_{grid} variation during P and Q changes.

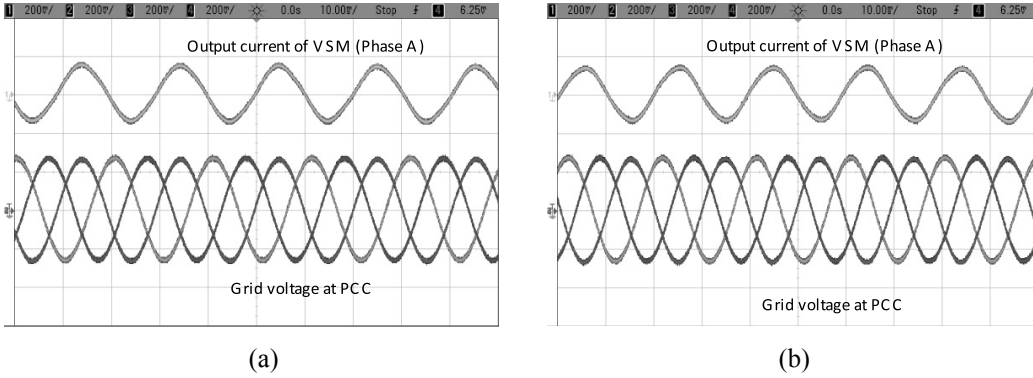


Fig. 8. Voltage and current (Phase ‘A’) waveforms when (a) P = 500 W (b) P = -500 W.

EFFECT OF VARIATION IN THE INERTIA VALUE ON THE POWER RESPONSE

The effect of variation in the value of inertia ($H=I/T_a$) on the power response is simulated and the performance is studied. When the value of inertia constant, H , of VSM increases, rise time in the response of output power decreases. The oscillations due to low frequency variations in the output power of VSM are eliminated by changing the value of H . However, delay time increases further as shown in Figure 9.

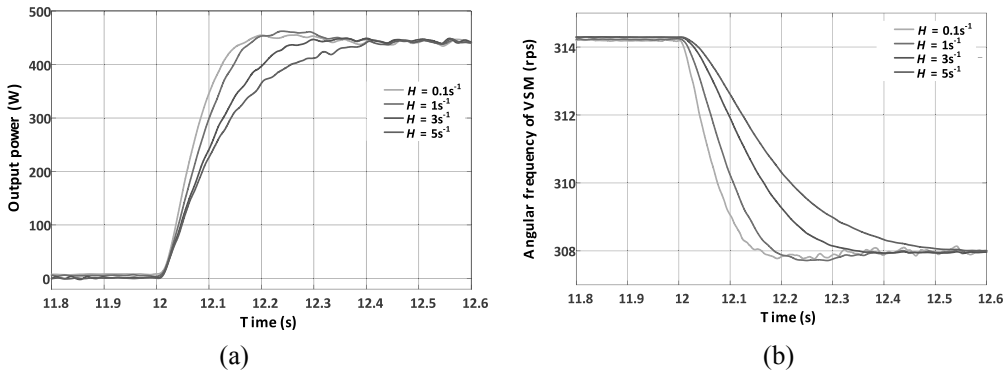


Fig. 9. Effect of inertial value on (a) Output power of VSM (b) Angular frequency.

COMPARISON OF VSM CONTROL WITH DROOP CONTROL

Load sharing among parallel connected synchronous generators is achieved using power versus frequency droop characteristics in the governor control. Droop control has been implemented in inverter based microgrids for load sharing among the parallel inverters. Studies conducted by different researchers show the similarities and differences in the droop controlled inverters and the VSM based control schemes (Arco et al., 2014; and Liu et al. 2016). It has been established from the studies that droop control can be considered as a special case of VSM control with zero inertia. Therefore droop control can only mimic the operation of governor in synchronous generator, while the VSM control mimics the inertial characteristics of the synchronous generators. In this section, the performance of the proposed VSM control is compared with the conventional power versus frequency based droop control method for inverters. The reference power generated from the droop control, P_{ref} , is given in Equation (22). The value of ω_{grid} is calculated by PLL in this droop control method.

$$P_{ref} = k_w(\omega_{ref}^* - \omega_{grid}) \tag{22}$$

When the frequency of the grid changes from 50 Hz to 51 Hz, droop control makes the inverter to absorb real power of 500 W from the grid. The output current of droop control for the increase in the grid frequency is shown in

Figure 10(a). Delay caused by PLL in the computation of ω_{grid} is reflected in the response of droop control because the reference power is generated from the frequency error in droop control. When the power is absorbed (negative power), the output current of VSC is phase shifted by 180° as shown in Figure 10(a). Similarly, the real power of 500 W is injected by the droop control when the grid frequency decreases from 50 Hz to 49 Hz as shown in Figure 10(b). The comparison in terms of output power response has been carried out between the VSM control and the existing droop control as shown in Figure 11(a). The VSM control gives less overshoot in output power response during frequency fluctuations. A steady state oscillation shall be observed in the real power injected into the grid by droop control as shown Figure 11(b). This fluctuation is due to the small error present in the computation of grid frequency by PLL. This oscillation may be worse when large sustained frequency variations occur in the grid. Thus it can be concluded that the VSM control gives a better response for inverters connected in weak grids, when compared to the conventional droop control.

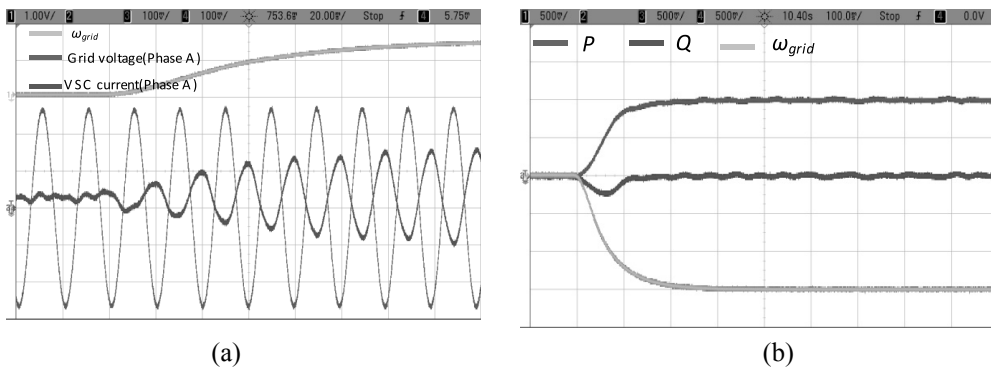


Fig. 10. (a) Droop control response to grid frequency rise from 50 Hz to 51 Hz; (b) P, Q and ω_{grid} of droop control for decrease in grid frequency from 50 Hz to 49 Hz.

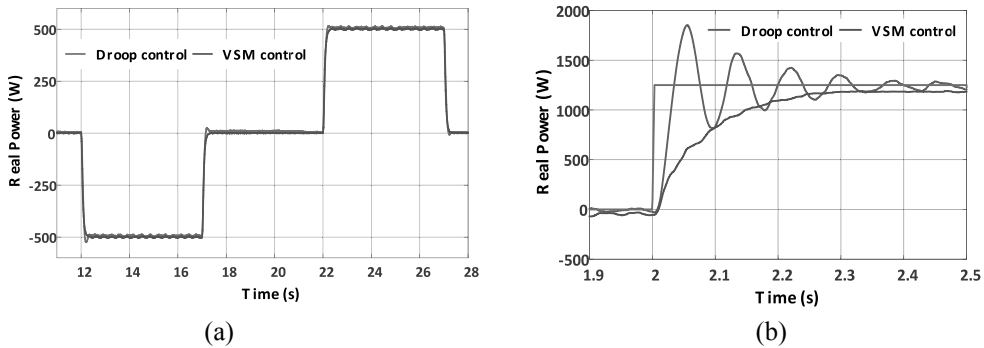


Fig. 11. (a) Real power response for small frequency change; (b) Real power response for large frequency change.

PERFORMANCE OF MODIFIED VSM CONTROL WITH CONVENTIONAL DROOP AND VSM CONTROL METHODS

According to the rotor motion equation of the synchronous machine, the acceleration of the machine is determined by the power balance equation with damping term, i.e., $k_d(\omega_{VSM} - \omega_{grid})$ (Case 1) as given in Equation (1). But the damping term contains ω_{grid} which is computed using a PLL unit. The PLL unit is not capable of tracking the value of frequency during sudden fluctuations in grid voltage. To understand the feasibility to eliminate the PLL from the VSM control, Equation (1) is modified by removing the damping term as given in Equation (23) and a case study is conducted on the experimental setup of the VSM (Case 2).

$$T_a \frac{d\omega_{VSM}}{dt} = P_m - P_e + k_w(\omega_{VSM}^* - \omega_{VSM}) \quad (23)$$

Experimental result of the VSM without damping term (Case 2) is compared with the VSM control with damping term (Case 1) as shown in Figure 12. When the damping term is removed in VSM control, some oscillations occur in the output power. This proves that the damping term helps the VSM control like the damper windings in the synchronous machine to control the output power without any oscillations. However, these oscillations present in Case 2 can be eliminated by increasing the integral gain, K_{i1} of the PI controller by a factor λ as expressed in Equation (24) (Case 3).

$$\delta = \left(K_{p1} + \frac{\lambda K_{i1}}{s} \right) (P_{VSM} - P_e) \quad (24)$$

The response of VSM for Case 3 is shown in Figure 12 for the value of $\lambda K_{i1} = 2.5$. The figure confirms that the response of VSM for both the Case 1 and Case 3 is almost the same. Hence, the PLL unit can be removed permanently from the VSM control. Though the PLL unit is successfully removed from the VSM control, the VSM control has a delay time (t_{d1}) of 0.20 s in both Case 1 and Case 3. To improve the speed of response of the VSM control, an attempt is made by adding a positive power term [$P_c = k_c(\omega_{VSM} - \omega_{grid})$] which acts as a compensation term for improving the speed of response in the rotor motion equation. Equation (23) is modified further as given in Equation (25) (Case 4). This VSM control is proposed as a modified VSM control.

$$T_a \frac{d\omega_{VSM}}{dt} = P_m - P_e + k_w(\omega_{VSM}^* - \omega_{VSM}) + k_c(\omega_{VSM} - \omega_{grid}) \quad (25)$$

Though the term ω_{grid} is used in Equation (25), a dedicated program is developed to compute the value of grid frequency using the zero crossing detection method. Hence, the rise time of the VSM control is improved as shown in Figure 12 for Case 4.

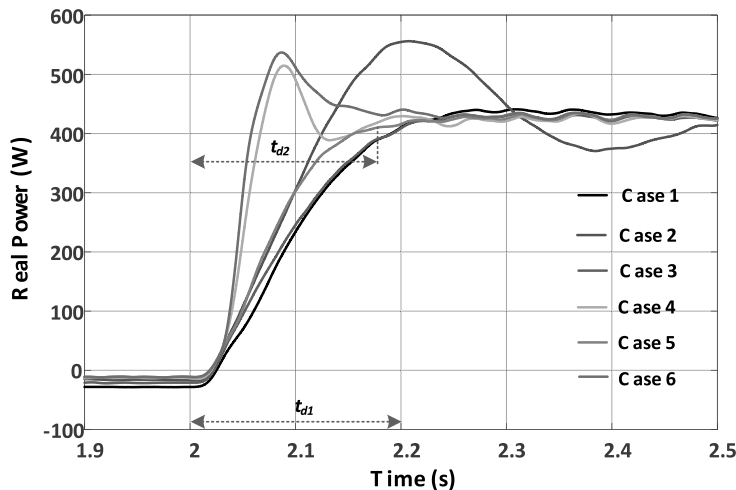


Fig. 12. Performance comparison for all six cases considered in the analysis.

The performance of the conventional droop control is shown in Figure 12 (Case 5). From the figure, it can be observed that there is a delay time (t_{d2}) of 0.18 s present in the conventional droop control. This delay is basically caused by the PLL unit in the computation of ω_{grid} . To eliminate this delay in the droop control method, the dedicated program used in Case 4 to compute the value of ω_{grid} is utilized. Hence, an attempt is made to remove the PLL in droop control method also (Case 6). The performance of the droop control which uses a dedicated program for

computing ω_{grid} is shown in Figure 12. Though the droop control without PLL shows slightly faster response than the modified VSM control (Case 4), there is a slight overshoot in the actual real power output of Case 6. However, the performance of the droop control completely depends on the value of grid frequency, which is computed by the dedicated program. The computation of the grid frequency may be poor during the transient events or in the presence of harmonics in the grid voltage. Hence, the proposed modified VSM control is more reliable than the droop control. The details of the different cases discussed in this section are summarised in Table 3.

Table 3. Summary of the different control cases for grid connected converters.

Case No.	Description	Remarks
Case 1	VSM control with the damping term [Equation (1)]	Standard
Case 2	VSM control without the damping term [Equation (23)]	Novel
Case 3	VSM control with increased K_{i1} of the PI controller [Equation (24)]	Novel
Case 4	Modified VSM control [Equation (25)]	Novel
Case 5	Conventional droop control with PLL [Equation (22)]	Standard
Case 6	Conventional droop control without PLL	Standard

CONCLUSIONS

The primary focus of this work was to develop a VSM control for the grid connected VSC's in the power system. The developed model of the VSM, which operates without a phase locked loop for grid synchronization, is simulated in the MATLAB/Simulink platform. The simulation study was performed for a DC voltage of 360 V, the grid voltage of 200 V rms (L-L), and grid frequency of 50 Hz. A hardware prototype of the VSM controlled grid connected VSC was set up in the laboratory environment and the controller was implemented in OPAL-RT real time simulator. The small signal model and the eigenvalue analysis of the overall system establish the stable operation of the VSM. The performance comparison between the hardware and simulation results shows the close match between them. To overcome the limitations of PLL in the droop control and conventional VSM control, a modified VSM is proposed to eliminate the dependency on PLL unit for frequency measurement. It can be concluded that the modified VSM controlled voltage source converter gives a better response over the conventional VSM control and droop control methods. Hence, the modified VSM control may be a suitable candidate for the power system applications.

REFERENCES

- Alipoor, J., Miura, Y. & Ise, T. 2015.** Power system stabilization using virtual synchronous generator with alternating moment of inertia. *IEEE Journal of Emerging and Selected Topics in Power Electronics* **3**(2): 451–458.
- Beck, H.P. & Hesse, R. 2007.** Virtual synchronous machine. 9th International Conference on Electrical Power Quality and Utilisation: 1–6.
- Bidram, A., Davoudi, A., Lewis, F.L. & Ge, S.S. 2014.** Distributed adaptive voltage control of inverter-based microgrids. *IEEE Transactions on Energy Conversion* **29**(4): 862–872.
- Chen, D., Xu, Y. & Huang, A.Q. 2017.** Integration of DC Microgrids as Virtual Synchronous Machines into the AC Grid. *IEEE Transactions on Industrial Electronics* **64**(9): 7455–7466.
- D'Arco, S., Suul, J.A. & Fosso, O.B. 2015.** A Virtual Synchronous Machine implementation for distributed control of power converters in SmartGrids. *Electrical Power Systems Research* **122**: 180–197.
- D'Arco, S. & Suul, J.A. 2014.** Equivalence of Virtual Synchronous Machines and Frequency-Droops for Converter-Based MicroGrids. *IEEE Transactions on Smart Grid* **5**(1): 394–395.
- Driesen, J. & Visscher, K. 2008.** Virtual synchronous generators. *IEEE Power and Energy Society General Meeting: Conversion*

and Delivery of Electrical Energy in the 21st Century: 1–3.

- Guan, M., Pan, W., Zhang, J. & Hao, Q. 2015.** Synchronous Generator Emulation Control Strategy for Voltage Source Converter (VSC) Stations. *IEEE Transactions on Power Systems* **30**(1): 1–9.
- Hirase, Y., Abe, K., Sugimoto, K., Sakimoto, K., Bevrani, H. & Ise, T. 2018.** A novel control approach for virtual synchronous generators to suppress frequency and voltage fluctuations in microgrids. *Applied Energy* **210**: 699–710.
- Liu, J., Miura, Y., Bevrani, H. & Ise, T. 2017.** Enhanced Virtual Synchronous Generator Control for Parallel Inverters in Microgrids. *IEEE Transactions on Smart Grid* **8**(5): 2268–2277.
- Liu, J., Miura, Y. & Ise, T. 2016.** Comparison of Dynamic Characteristics Between Virtual Synchronous Generator and Droop Control in Inverter-Based Distributed Generators. *IEEE Transactions on Power Electronics* **31**(5): 3600–3611.
- Mishra, S., Pullaguram, D., Achary Buragappu, S. & Ramasubramanian, D. 2016.** Single-phase synchronverter for a grid-connected roof top photovoltaic system. *IET Renewable Power Generation* **10**(8): 1187–1194.
- Pertl, M., Weckesser, T., Rezkalla, M. & Marinelli, M. 2017.** Transient stability improvement: A review and comparison of conventional and renewable-based techniques for preventive and emergency control. *Electrical Engineering*: 1–18.
- Pogaku, N., Prodanović, M. & Green, T.C. 2007.** Modeling, analysis and testing of autonomous operation of an inverter-based microgrid. *IEEE Transactions on Power Electronics* **22**(2): 613–625.
- Tielens, P. & Hertem, D. Van. 2016.** The relevance of inertia in power systems. *Renewable and Sustainable Energy Reviews* **55**: 999–1009.
- Torres L., M.A., Lopes, L.A.C., Moran T., L.A. & Espinoza C., J.R. 2014.** ‘Self-Tuning Virtual Synchronous Machine: A Control Strategy for Energy Storage Systems to Support Dynamic Frequency Control. *IEEE Transactions on Energy Conversion* **29**(4): 833–840.
- Wu, H., Ruan, X., Yang, D., et al. 2016.** Small-Signal Modeling and Parameters Design for Virtual Synchronous Generators. *IEEE Transactions on Industrial Electronics* **63**(7): 4292–4303.
- Zhong, Q.C., Nguyen, P.L., Ma, Z. & Sheng, W. 2014.** Self-synchronized synchronverters: Inverters without a dedicated synchronization unit. *IEEE Transactions on Power Electronics* **29**(2): 617–630.
- Zhong, Q.C. & Weiss, G. 2011.** Synchronverters: Inverters that mimic synchronous generators. *IEEE Transactions on Industrial Electronics* **58**(4): 1259–1267

Submitted: 27/12/2017

Revised: 12/10/2018

Accepted: 19/10/2018

تحكم افتراضي في الجهاز المتزامن لمحاولات الطاقة الكهربائية المتصلة بالشبكة لتطبيقات نظام الطاقة

*كومارافيل س، *فينو توماس، *تيرينس أودونيل و*أشوك إس
*معهد كاليكوت الوطني للتكنولوجيا، كيرالا، الهند
**كلية جامعة دبلن، بلفيلد، دبلن، أيرلندا

الخلاصة

أصبحت مولدات الطاقة الموزعة القائمة على الطاقة المتجددة جزءاً لا يتجزأ من أنظمة الطاقة المستقبلية. تلعب محاولات الطاقة الإلكترونية دوراً رئيسياً كأجهزة بينية بين مصادر الطاقة المتجددة وشبكة المرافق. نظراً لأن محاولات الطاقة الإلكترونية لا تمتلك أي محادثة دورية مثل المولد المتزامن، فإن التقلبات السريعة في إمدادات الطاقة والطلب عليها تتسبب في انحرافات مفاجئة في تيرة المحول الإلكتروني الذي يسيطر على شبكات الطاقة الضعيفة. يحاول نهج الجهاز الافتراضي المتزامن (VSM) للتحكم في المحولات المتصلة بالشبكة تقليد سلوك الجهاز المتزامن ويوفر المحادثة الذاتية للشبكة بسبب التخزين الكهربائي. في هذا البحث، تم اقتراح استراتيجية مُعدلة للتحكم في VSM تعتمد على معادلة التارجح لمحاولات متصلة بشبكة ثلاثية الأطوار. تم تطبيق استراتيجية التحكم المقترحة في إطار مرجعي ثابت ولا تحتاج إلى حلقة مغلقة الطور لمزامنة الشبكة على عكس العديد من الطرق الموجودة في المنشورات الأخرى. تتكون وحدة VSM من وحدة تخزين DC متصلة من خلال محول لمصدر جهد ثلاثي الأطوار مع فلتر LCL في الشبكة ونظام التحكم المحلي المماثل. تم تطوير الإعداد لاختبار وحدة VSM بمواصفات 200 فولت، 50 هرتز و 1 كيلو فولت أمبير في المختبر للتحقق من صحة خطة التحكم. وقد أجريت دراسات مختلفة للأداء مثل التحكم الحقيقي والتفاعلي في الطاقة وتأثير التباين في قيمة القصور الذاتي في VSM وعلى استجابة الطاقة واستجابة VSM لتغير تردد الشبكة.

تمت مقارنة أداء التحكم في VSM مع طريقة التحكم التقليدية في التدلي للمحولات المتصلة بالشبكة. وأثبتت النتائج أن مخطط التحكم المعدل في VSM يوفر أداءً أفضل من التحكم التقليدي في التدلي.